Reaction of the Diimine Pyridine Ligand with Aluminum Alkyls: An Unexpectedly Complex Reaction

Quinten Knijnenburg,† Jan M. M. Smits,† and Peter H. M. Budzelaar*,‡

Institute for Molecular Materials, Radboud University Nijmegen, Toernooiveld 1, 6525 ED Nijmegen, The Netherlands, and Department of Chemistry, University of Manitoba, Winnipeg, MB, R3T 2N2, Canada

Received October 31, 2005

The diimine pyridine ligand 2,6-{2,6-^{i}Pr$_2$C$_6$H$_3$N═CMe}$_2$C$_5$H$_3$N (**1**) was reacted with a series of aluminum alkyls (Me$_3$Al, Et$_3$Al, ^{i}Bu$_3$Al, ^{i}Bu$_2$AlH, Et$_2$AlCl). Depending on the choice of alkyl, addition to the imine carbon and the pyridine C2 and C4 positions was observed. Addition to C2 usually dominates but is reversible; the C4 alkylation product eventually dimerizes via double C−C coupling. Reaction of **1** with AlCl$_3$ gave the ionic complex [**1**·AlCl$_2$]$^+$[AlCl$_4$]$^-$. DFT calculations were used to support NMR assignments of the various addition products and also to study alkyl transfer from Et$_2$AlCl to simplified model ligand **1′**. Direct alkyl transfer from coordinated Et$_2$AlCl to the ligand C4 position is not possible. Introduction of a second molecule of Et$_2$AlCl results in formation of the ion pair [**1′**·AlEtCl]$^+$[Et$_3$AlCl]$^-$, from which alkyl transfer to any position of the ligand is relatively easy. The dimerization of the C4-alkylated product is symmetry-forbidden and was calculated to follow a stepwise biradical path with an unusually low barrier.

Introduction

Since the parallel discovery by the groups of Brookhart and Gibson of the performance of iron and cobalt complexes bearing diimine pyridine ligands in olefin oligomerization and polymerization,[1] numerous studies have been dedicated to this particular ligand. In the case of cobalt, we and others showed that MAO achieves reduction of the dichloride complex, prior to alkylation in the activation pathway.[2] For iron, dialkyl complexes can be formed under the right circumstances,[3,4] but reduction of the metal center[3,5] and (reversible) attack of alkyl groups on the ligand framework[3] have also been observed. Furthermore, aluminum alkyls can displace the iron atom partially or completely[6] from the ligand. Ligand alkylation has also been observed with the transition metals Ti,[7] V,[8] and Cr[9] (in combination with various alkylating agents) and with the main-group metals Li,[10] Al,[11,12] Zn, and Mg.[13] Alkylation can occur at various positions of the ligand framework: so far, examples of alkyl attack at the imine carbon,[3,11,12] the pyridine C2[3,7,8] and C4,[9] and nitrogen atoms[10,13] have been reported, as well as double alkylation (at both C2 and C3 atoms).[8] While for this particular system ligand-centered reactivity has only recently attracted attention, chemical noninnocence of the related α-diimine and imine-pyridine systems has been known for a long time.[14] A recent report shows that also for these ligands alkylation can be reversible.[15]

The reaction of aluminum alkyls with diimine pyridine ligands is particularly important for two reasons. In the first place, aluminum alkyls are the cocatalysts of choice for activating transition metal complexes of diimine pyridine ligands in olefin polymerization[16] and hydrogenation.[17] Secondly, the products of the reaction of aluminum alkyls with this ligand have been reported to generate transition-metal-free olefin polymerization catalysts on activation with Lewis acids.[11]

* Corresponding author. E-mail: budzelaa@cc.umanitoba.ca.
† Radboud University.
‡ University of Manitoba.

(1) (a) Small, B. L.; Brookhart, M.; Bennett, A. A. *J. Am. Chem. Soc.* **1998**, *120*, 4049. (b) Britovsek, G. J. P.; Gibson, V. C.; Kimberley, B. S.; Maddox, P. J.; McTavish, S. J.; Solan, G. A.; White, A. J. P.; Williams, D. J. *Chem. Commun.* **1998**, 849. (c) Small, B. L.; Brookhart, M. *J. Am. Chem. Soc.* **1998**, *120*, 7143. (d) Britovsek, G. J. P.; Bruce, M.; Gibson, V. C.; Kimberley, B. S.; Maddox, P. J.; Mastroianni, S.; McTavish, S. J.; Redshaw, C.; Solan, G. A.; Strömberg, S.; White, A. J. P.; Williams, D. J. *J. Am. Chem. Soc.* **1999**, *121*, 8728.

(2) (a) Kooistra, T. M.; Knijnenburg, Q.; Smits, J. M. M.; Horton, A. D.; Budzelaar, P. H. M.; Gal, A. W. *Angew. Chem., Int. Ed.* **2001**, *40*, 4719. (b) Gibson, V. C.; Humphries, M.; Tellmann, K.; Wass, D.; White, A. J. P.; Williams, D. J. *Chem. Commun.* **2001**, 2252.

(3) Scott, J.; Gambarotta, S.; Korobkov, I.; Budzelaar, P. H. M. *J. Am. Chem. Soc.* **2005**, *127*, 13019.

(4) Bouwkamp, M. W.; Lobkovsky, E.; Chirik, P. J. *J. Am. Chem. Soc.* **2005**, *127*, 9660.

(5) Bouwkamp, M. W.; Bart, S. C.; Hawrelak, E. J.; Trovitch, R. J.; Lobkovsky, E.; Chirik, P. J. *Chem. Commun.* **2005**, 3406.

(6) Scott, J.; Gambarotta, S.; Korobkov, I.; Knijnenburg, Q.; De Bruin, B.; Budzelaar, P. H. M. *J. Am. Chem. Soc.*, submitted.

(7) Calderazzo, F.; Englert, U.; Pampaloni, G.; Santi, R.; Sommazzi, A.; Zinna, M. *J. Chem. Soc., Dalton Trans.* **2005**, 914.

(8) Reardon, D.; Conan, F.; Gambarotta, S.; Yap, G.; Wang, Q. *J. Am. Chem. Soc.* **1999**, *121*, 9318.

(9) Sugiyama, H.; Aharonian, G.; Gambarotta, S.; Yap, G. P. A.; Budzelaar, P. H. M. *J. Am. Chem. Soc.* **2002**, *124*, 12268.

(10) (a) Khorobkov, I.; Gambarotta, S.; Yap, G. P. A.; Budzelaar, P. H. M. *Organometallics* **2002**, *21*, 3088. (b) Clenthsmith, G. K. B.; Gibson, V. C.; Hitchcock, P. B.; Kimberley, B. S.; Rees, C. W. *Chem. Commun.* **2002**, *14*, 1498.

(11) Bruce, M.; Gibson, V. C.; Redshaw, C.; Solan, G. A.; White, A. J. P.; Williams, D. J. *Chem. Commun.* **1998**, *18*, 2523.

(12) Milione, S.; Cavallo, C.; Tedesco, C.; Grassi, A. *J. Chem. Soc., Dalton Trans.* **2002**, *8*, 1839.

(13) Blackmore, I. J.; Gibson, V. C.; Hitchcock, P. B.; Rees, C. W.; Williams, D. J.; White, A. J. P. *J. Am. Chem. Soc.* **2005**, *127*, 6012.

(14) (a) Klerks, J. M.; Stufkens, D. J.; Van Koten, G.; Vrieze, K. *J. Organomet. Chem.* **1979**, *181*, 271. (b) Van Koten, G.; Jastrzebski, J. T. B. H.; Vrieze, K. *J. Organomet. Chem.* **1983**, *250*, 49.

(15) Riollet, V.; Copéret, C.; Basset, J.-M.; Rousset, L.; Bouchu, D.; Grosvalet, L.; Perrin, M. *Angew. Chem., Int. Ed.* **2002**, *41*, 3025.

(16) Liu, J.; Li, Y.; Liu, J.; Li, Z. *Macromolecules* **2005**, *38*, 2559.

(17) (a) Horton, A. D.; Knijnenburg, Q.; Van der Heijden, H.; Budzelaar, P. H. M.; Gal, A. W. WO 03042131 (2003); EP 2001-204376 (2001). (b) Knijnenburg, Q.; Horton, A. D.; Van der Heijden, H.; Kooistra, T. M.; De Bruin, B.; Hetterscheid, D. G. H.; Smits, J. M. M.; Budzelaar, P. H. M.; Gal, A. W. *J. Mol. Catal. A-Chem.* **2005**, *232*, 151.

10.1021/om050936m CCC: $33.50
Publication on Web 01/21/2006

Scheme 1. Ligand 1

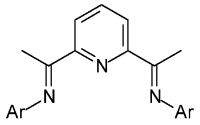

1

Ar = 2,6-*i*Pr$_2$C$_6$H$_3$

Scheme 2. Alkylation Product Types Observed in This Work

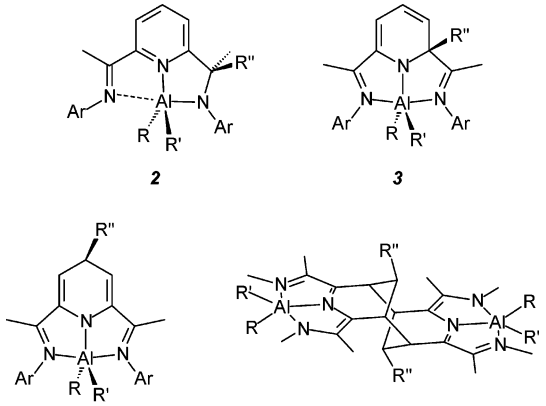

2 *3* *4* *5*

a: R = R' = R'' = Me
b: R = R' = R'' = Et
c: R = R' = R'' = *i*Bu
d: R = Cl, R' = R'' = Et
e: R = R' = *i*Bu, R'' = H
f: R = R' = Me, R'' = H

Scheme 3. Alternative Alkylation Product Types Considered but Not Observed in This Work

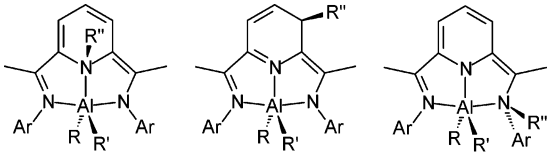

6 *7* *8*

For these reasons, we decided to study the reactions of ligand **1** (Scheme 1) with several aluminum alkyls in detail. Gibson reacted both **1** and related bis(aldimine) pyridine ligands with aluminum alkyls and from these reactions obtained the products of addition to the imine C═N bond in pure form.[11] Milione studied the reaction of **1** with Et_2AlCl[12] and mentions complexation and alkylation at the imine carbon as the main or sole reactions occurring. As we will show below, the reaction is much more complicated than indicated by these earlier studies and features alkyl addition to at least three positions of the ligand as well as dimerization of one of the alkylation products. Depending on the choice of alkyl and reaction conditions, we have observed alkylation at the imine position (**2**) and at pyridine C2 (**3**) or C4 (**4**) as well as dimerization of **4** to its polycyclic dimer **5** (see Scheme 2). Part of this work has been communicated.[18]

Additional alkylation products could in principle be formed, as shown in Scheme 3. As mentioned above, products analogous to **6** have been observed for Li,[10] Mg, and Zn;[13] alkylation at C3 (without preceding C2 alkylation: **7**) or at the imine nitrogen (**8**) has not been reported so far. We will be considering these alternative products in the theoretical parts of this paper.

(18) Knijnenburg, Q.; Smits, J. M. M.; Budzelaar, P. H. M. *C. R. Chimie* **2004**, *7*, 865.

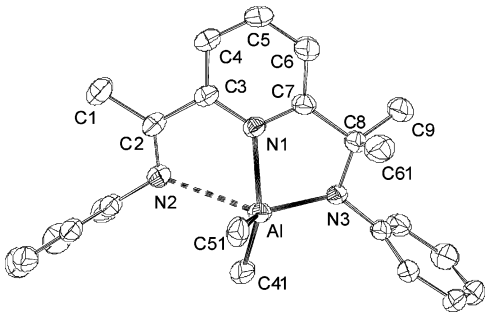

Figure 1. Thermal ellipsoid plot of **2a** (50% probability). Hydrogen atoms and isopropyl groups are omitted for clarity.

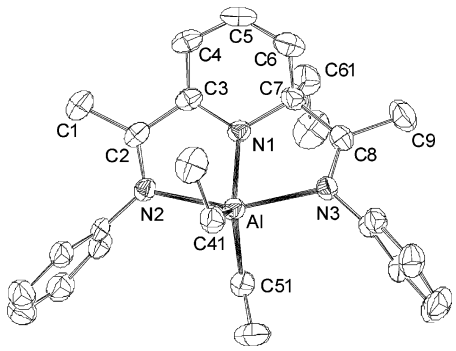

Figure 2. Thermal ellipsoid plot of **3b** (50% probability). Hydrogen atoms and isopropyl groups are omitted for clarity.

Results and Discussion

We have investigated the stoichiometric reactions of aluminum alkyls with the free ligand **1**. In all of these reactions, a mixture of products is formed initially. Prolonged heating changes the composition of the mixture, but never in such a way that only a single product remains. Thus, pure compounds could only be obtained in those cases where a single product crystallized preferentially (other separation techniques failed). Fortunately, we were able to isolate pure samples of a C2 alkylation product (**3b**) and two dimers of C4 alkylation products (**5d**,[18] **5e**) in this way. One imine alkylation product (**2d**) was also obtained in crystalline form, but not in sufficient quantities for NMR characterization;[18] therefore, we prepared pure samples of **2a** and **2b** following the route previously reported by Gibson,[11] using excess aluminum alkyl. Comparison of the spectra of purified **2** and **3** with those of the reaction mixtures allowed easy assignment of such alkylation products in all mixtures. The C4 alkylation products could not be isolated pure because they dimerize slowly as they are formed. They have, however, very characteristic signals for the (former) pyridine ring protons, which make assignment straightforward. As a further support for the NMR assignments, we calculated ^{1}H and ^{13}C NMR shifts for the various products (potentially) formed with Me_3Al and Et_3Al using the GIAO method. In the following sections, we first discuss the pure compounds we managed to isolate and the assignment of their spectra and then use these to interpret the progress of the addition reactions.

Individual Alkylation Products.

Imine Alkylation: 2. Pure samples of complexes **2a** and **2b**, for use as reference materials in the analysis of mixture spectra, were prepared by the method of Gibson[11] (treating **1** with 2 equiv of Me_3Al or Et_3Al, 12 h of reflux in toluene, removal of the solvent, crystallization from toluene). We also

Table 1. Calculated and Observed Chemical Shifts for 3b

	^{1}H		^{13}C	
position	calc	obs	calc	obs
Py 2			73.4	67.5
Py 3	5.12	5.12	114.4	101.7
Py 4	6.33	6.29	134.3	126.2
Py 5	5.71	5.66	105.6	114.2
Py 6			152.5	146.2
2-*CH*$_2$Me	2.86, 0.97	2.4, 1.3	35.9	28.6[a]
2-CH$_2$*Me*	1.08	0.9	9.3	6.2
C(Me)═N			194.1, 181.7	183.1, 173.8
C(*Me*)═N	2.05, 2.03	1.75, 1.55	23.2, 19.4	17.9, 16.8
Al*CH*$_2$Me	−0.13, −0.14, −0.20, −0.33	0.25−0.0	4.7, 1.7	1.4, −0.5
AlCH$_2$*Me*	0.98, 0.31	1.19, 0.74	13.6, 11.9	10.8, 8.7
Ar *i*,*o*			150.3, 150.2, 147.5, 147.6, 146.7, 146.5	143.2, 143.0, 141.1, 140.5, 140.0, 140.0
Ar *m*,*p*	7.14, 7.13, 7.12, 7.09, 7.09, 7.02	7.1	130.8, 130.5, 129.9, 129.5, 129.0, 128.6	126.7, 126.5, 124.6, 124.5, 124.4, 123.8
Ar *CH*Me$_2$	3.15, 2.87, 2.76, 2.60	3.21, 3.09, 3.07, 3.01	33.5, 33.3, 32.2, 32.1	28.3, 27.7, 27.7, 27.5[a]
Ar CH*Me*$_2$	1.45, 1.32, 1.28, 1.25, 1.07, 1.06, 0.97, 0.90	1.41, 1.41, 1.39, 1.37, 1.11, 1.00, 0.99, 0.97	28.0, 27.8, 27.3, 26.7, 26.3, 25.5, 24.3, 24.0	26.0, 25.4, 25.0, 25.0, 24.9, 24.1, 23.7, 23.1

[a] Assignment tentative.

Table 2. Calculated and Observed Characteristic ^{1}H Resonances for Various Complexes

complex	position	calc	obs
1	Py 3,5	8.76	8.40
	Py 4	7.86	7.22
2a	Ar C*H*Me$_2$	3.69, 2.84	3.97, 2.94
3a	Py 3	5.05	5.16
	Py 4	6.29	6.32
	Py 5	5.77	5.74
4a	Py 3,5	5.10	5.03
	Py 4	3.92	3.52
6a	Py 3,5	6.56	*a*
	Py 4	4.88	*a*
7a	Py 3	3.54	*a*
	Py 4	5.49	*a*
	Py 5	6.38	*a*
8a	Py 3	6.33	*a*
	Py 4	4.94	*a*
	Py 5	5.64	*a*
2b	Ar C*H*Me$_2$	3.88, 3.72, 2.50, 2.70	4.38, ...
3b	Py 3	5.12	5.12
	Py 4	6.33	6.29
	Py 5	5.71	5.66
4b	Py 3,5	5.18	5.03
	Py 4	3.76	3.7
4f	Py 3,5	5.03	4.94
	Py 4	3.97	3.53
(κ^3-**1**)AlCl$_2^+$	Py 3,5	8.15	7.92
	Py 4	8.60	8.63
(κ^1-im-**1**)AlMe$_3$	Py 3	7.35	*a*
	Py 4	7.75	*a*
	Py 5	8.65	*a*
(κ^1-py-**1**)AlMe$_3$	Py 3,5	8.57	*a*
	Py 4	7.90	*a*

[a] No signals attributable to these compound were observed in any spectra.

Table 3. Composition of Reaction Mixture of 1 with Al Alkyls, Immediately after Mixing, in mol %

Al alkyl	**2**	**3**	**4**
Me$_3$Al (**a**)	66	29	3[a]
Et$_3$Al (**b**)	17	55	28
Et$_2$AlCl (**d**+**d′**)	9	78	13
^{i}Bu$_3$Al (**c**)			6[b]
^{i}Bu$_2$AlH (**e**)			≈100

[a] Plus ca. 2 mol % **4f**. [b] Plus ca. 1 mol % of **4e** and ca. 3 mol % of a second 4-^{i}Bu alkylation product; remainder appears to consist of coordination complex(es) of **1**.

Table 4. Calculated Relative Stabilities (kcal/mol) for Reaction Products of 1 with Me$_3$Al and Et$_3$Al

product	RIDFT-bp86/SV(P)	B3LYP/6-311G**[a]
2a	13.2	9.0
3a	13.6	10.8
4a	2.6	(0)
6a	20.4	22.1
7a	(0)	2.0
8a	27.0	29.0
2b	16.5	15.5
3b	14.5	15.0
4b	(0)	(0)
5b	−15.3	−4.8

[a] At RIDFT-bp86/SV(P) geometries.

determined the structure of **2a** (Figure 1; for bond lengths in this and other complexes, see Table 6); its geometry is fully comparable to the analogous product of the reaction between an aldimine ligand and AlMe$_3$ as reported by Gibson.[11] The central Al is tetrahedral with a short Al−N3 bond (1.878(3) Å) because N3 has now become anionic; the Al−N2 distance is very long (2.591(5) Å) and probably does not represent a real coordination bond.

Compared to complexes **3** and **4** and the free ligand **1**, complexes **2** show a characteristic low-field isopropyl methine resonance, which (according to NOESY and calculations mentioned below) is due to an isopropyl group on the "reacted" side of the complex. Apart from this, they show no resonances that allow easy identification and quantification in mixtures.

From the reaction of **1** with Et$_2$AlCl, we were able to isolate a few orange crystals of complex **2d** by "crystal picking". Although the quality of the crystals was poor, the connectivity of the ligand framework could be confirmed by X-ray diffraction.[18]

Pyridine C2 Alkylation: 3. Pure samples of **3b** could be obtained by reacting **1** with Et$_3$Al at room temperature in hexane, cooling to −30 °C, and washing with cold hexane. According to ^{1}H NMR (see below and Table 3), **3b** is initially formed in about 55% yield, but the above partial crystallization and washing procedure obviously results in significant losses, and the isolated yield of **3b** is typically about 10%.

The ^{1}H NMR spectrum of **3b** shows three characteristic olefinic resonances for the (former) pyridine ring protons in the region of 5.0−7.0 ppm, with clear couplings between them. The aromatic, methine, and methyl resonances are unremarkable.

Table 5. Crystal Data and Structure Analysis Results

	2a	3b	5e	9
cryst color	translucent brown-red	transparent dark yellow-brown	dark red	transparent light yellow
cryst shape	rough fragment	regular thick platelet	regular fragment	rough fragment
cryst size (mm)	0.31 × 0.31 × 0.22	0.32 × 0.23 × 0.10	0.19 × 0.16 × 0.13	0.19 × 0.13 × 0.10
emp formula	$C_{46.50}H_{64}AlN_3$	$C_{39}H_{58}AlN_3$	$C_{82}H_{124}Al_2N_6$	$C_{40}H_{51}Al_2Cl_6N_3$
fw	691.99	595.86	1247.83	840.50
temp (K)		208(2)		
radiation/wavelength (Å)		Mo Kα (graphite monochromated)/0.71073		
cryst syst space group	triclinic $P\bar{1}$	triclinic $P1$	monoclinic $P2_1/c$	monoclinic $P2_1/n$
no. of reflns for cell	42	40	70	110 254
a (Å)	9.6818(6)	12.8955(15)	10.653(3)	24.292(5)
b (Å)	10.8761(7)	16.811(3)	16.9159(15)	13.808(3)
c (Å)	21.6405(17)	17.1893(19)	21.622(3)	27.336(5)
α (deg)	100.973(6)	87.810(19)	90	90
β (deg)	99.380(5)	79.367(11)	95.783(16)	102.06(3)
γ (deg)	104.004(5)	89.436(18)	90	90
volume (Å^3)	2117.7(3)	3659.7(9)	3876.7(13)	8966(3)
Z, d_{calc} (Mg/m^3)	2, 1.085	4, 1.081	2, 1.069	8, 1.245
abs coeff (mm^{-1})	0.081	0.084	0.082	0.453
diffractometer/scan		Nonius KappaCCD with area detector θ and ω scan		
F(000)	754	1304	1368	3520
θ range for data collection (deg)	2.22 to 25.00	3.07 to 24.00	3.06 to 25.00	4.51 to 22.00
index ranges	$-11 \le h \le 11$ $-12 \le k \le 12$ $-25 \le l \le 25$	$-14 \le h \le 14$ $-19 \le k \le 19$ $-19 \le l \le 19$	$-12 \le h \le 12$ $-20 \le k \le 20$ $-25 \le l \le 25$	$-25 \le h \le 25$ $-14 \le k \le 14$ $-28 \le l \le 28$
reflns collected/unique	25 674/7437 [R_{int} = 0.0474]	98 451/11 472 [R_{int} = 0.1142]	65 449/6811 [R_{int} = 0.1215]	11 0254/10903 [R_{int} = 0.1279]
no. of obsd reflns ([$I_o > 2\sigma(I_o)$])	4772	7568	500	7112
abs corr		SADABS multiscan correction[46]		
refinement		full-matrix least-squares on F^2		
computing		SHELXL-97[47]		
no. of data/restraints/params	7437/15/483	11 472/0/801	6811/0/420	10 903/0/941
goodness-of-fit on F^2	1.032	1.099	1.068	1.042
SHELXL-97 weight params	0.0633, 2.4332	0.0347, 3.4821	0.0771, 3.5378	0.0912, 48.6697
final R indices	R1 = 0.0701	R1 = 0.0749	R1 = 0.0728	R1 = 0.0968
[$I > 2\sigma(I)$]	wR2 = 0.1544	wR2 = 0.1271	wR2 = 0.1737	wR2 = 0.2133
R indices	R1 = 0.1220	R1 = 0.1251	R1 = 0.1022	R1 = 0.1474
(all data)	wR2 = 0.1802	wR2 = 0.1431	wR2 = 0.1916	wR2 = 0.2422
largest diff peak and hole (e/Å^3)	0.782 and −0.371	0.223 and −0.242	0.529 and −0.402	1.757 and −1.457

Table 6. Selected Bond Distances (Å) and Angles (deg)

	2a	3b	5e	9
Al−N(1)	2.036(2)	1.885(3)	2.010(2)	1.958(6)
Al−N(2)	2.591(5)	2.240(3)	2.147(2)	2.083(6)
Al−N(3)	1.878(3)	2.221(3)	2.120(2)	2.076(6)
Al−C(41)	1.967(3)	1.980(4)	2.026(2)	
Al−C(51)	1.979(3)	1.981(4)	2.010(3)	
C(1)−C(2)	1.497(5)	1.504(4)	1.493(4)	1.500(11)
C(2)−N(2)	1.283(4)	1.284(4)	1.312(3)	1.289(9)
C(2)−C(3)	1.476(5)	1.475(5)	1.436(4)	1.471(11)
C(3)−N(1)	1.355(4)	1.366(4)	1.333(3)	1.322(9)
C(3)−C(4)	1.379(4)	1.364(5)	1.503(3)	1.396(11)
C(4)−C(5)	1.380(5)	1.433(5)	1.527(4)	1.370(12)
C(5)−C(6)	1.371(5)	1.333(5)	1.535(4)	1.374(12)
C(6)−C(7)	1.389(4)	1.513(5)	1.508(3)	1.391(11)
C(7)−N(1)	1.331(4)	1.455(4)	1.347(3)	1.338(10)
C(7)−C(8)	1.513(4)	1.516(5)	1.415(4)	1.475(11)
C(8)−C(9)	1.544(5)	1.506(5)	1.502(4)	1.487(11)
C(8)−N(3)	1.463(4)	1.278(4)	1.317(3)	1.286(9)
C(8)−C(61)	1.526(5)			
C(7)−(C61)		1.561(5)		
C(4)−C(6)#1			1.557(4)	
Al−Cl(1)				2.121(3)
Al−Cl(2)				2.112(3)
N(2)−Al−N(3)		152.34(11)	146.71(9)	149.4(3)
N(1)−Al−C(41)	138.63(14)	114.25(14)	142.35(12)	
N(1)−Al−C(51)	97.82(13)	133.02(14)	102.14(11)	
C(41)−Al−C(51)	114.25(17)	112.70(16)	115.31(13)	
N(1)−Al−Cl(1)				101.5(2)
N(1)−Al−Cl(2)				146.2(2)
Cl(1)−Al−Cl(2)				112.29(13)

The crystal structure of **3b** contains two independent molecules. Figure 2 shows one of these, and Table 6 gives geometrical parameters for it; full details for both molecules can be found in the Supporting Information. Because of the addition, the former pyridine ring is no longer planar, and the negative charge is localized on its nitrogen atom. This produces a short Al−N1 bond (1.885(3) Å) and localized pyridine double bonds (1.364(5) and 1.333(5) Å); the localization is somewhat less pronounced than in the vanadium-containing C2 alkylation product reported by Gambarotta.[8] The geometry around the central Al atom is distorted square pyramidal.

Pyridine C4 Alkylation Followed by Dimerization: 4 and 5. Mixtures of **1** and various aluminum alkyls frequently showed a characteristic doublet at 4.9 ppm (coupled to a less distinctive multiplet around 3.5 ppm) and/or two triplets at 4.8 and 3.5 ppm, each with a coupling of about 3.8 Hz. We assign these to the products **4** of addition to the pyridine C4 position of an alkyl group or a hydride, respectively. In most spectra, the amounts of these products are small, but in the reaction of Et_3Al with **1** complex **4b** can comprise up to 25 mol % of the product mixture. We were unable to isolate any complexes of this type in pure form. Our assignment is based on the following arguments:

- The shift and coupling are similar to those observed previously for a C4 hydride addition product containing Rh[19] and to shifts and couplings reported for more "normal" 4-hydropyridyl units.[20]
- From the reaction of Et_2AlCl with **1**, we were able to isolate and characterize *dimer **5d*** of C4 alkylation product **4d**.[18]

(19) Kooistra, T. M.; Hetterscheid, D. G. H.; Schwartz, E.; Knijnenburg, Q.; Budzelaar, P. H. M.; Gal, A. W. *Inorg. Chim. Acta* **2004**, *357*, 2945.

(20) See e.g.: Kita, Y.; Maekawa, H.; Yamasaki, Y.; Nishiguchi, I. *Tetrahedron* **2001**, *57*, 2095.

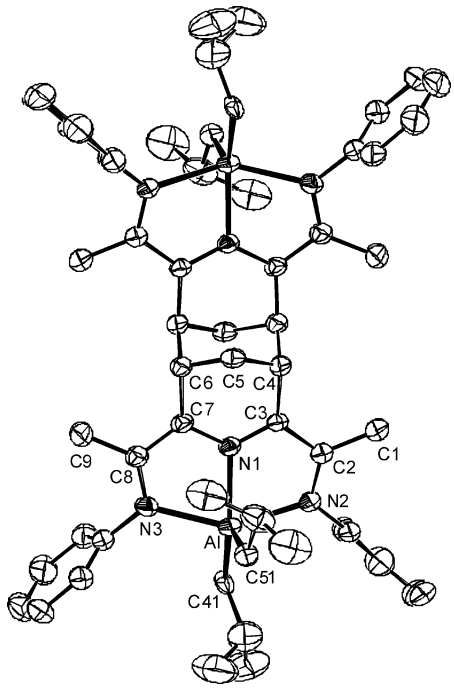

Figure 3. Thermal ellipsoid plot of **5e** (50% probability). Hydrogen atoms and isopropyl groups are omitted for clarity.

• A spectrum recorded immediately after mixing **1** and $^{i}Bu_2AlH$ appears to consist of mainly **4e**, with no other complexes recognizable in solution. A crystal obtained from this solution was of very poor quality, but X-ray structure determination confirmed its connectivity (see Supporting Information). From the mixture, we were able to isolate dimer **5e** after heating and workup.

• The shifts of the H3,5 protons and (where assignable) the H4 protons show satisfactory agreement with the calculated shifts.

The X-ray structures of **5d**[18] and **5e** (Figure 3) show a tricyclic ligand skeleton, similar to that reported by Gambarotta for the product of the reaction of **1**·$CrCl_3$ with BzMgCl.[9] In **5d**, as in the Cr analogue, the alkyl groups added to the ligand C4 position of each pyridyl unit avoid the second monomer unit. The Al atoms are five-coordinate with the usual square pyramidal geometry.

Neither **5d** nor **5e** gave an acceptable ^{1}H NMR spectrum in benzene, toluene, or any other solvent we tested. This might be simply due to their surprisingly low solubility. However, the intense purple color of the complexes in the solid state and as dilute toluene solutions suggests that easy formation of paramagnetic species might also play a role.

Calculation of NMR Shifts. Given the impossibility of separating isomeric complexes obtained in most reactions of aluminum alkyls with **1**, we decided to obtain more support for the NMR assignments of the various isomeric structures through prediction of the expected ^{1}H and ^{13}C NMR shifts. For "ordinary" organic compounds, shift prediction based on reference molecules, group contributions, and empirical corrections[21] is probably the most reliable method available at present. For the present cases, involving organometallic complexes with unusual and highly delocalized anionic ligands, such a procedure cannot be used, and we resorted to calculations,[22] using the GIAO method[23] (as implemented in Gaussian98[24]) at the B3LYP[25]/6-311G**[26] level. Perfect agreement is not expected for several reasons.[27] Nevertheless, we hoped that calculated data might be good enough to aid spectrum interpretation and assignments. Table 1 compares all calculated and observed shifts for complex **3b**. Table 2 lists calculated and observed shifts of complexes **2a**−**4a**, **6a**−**8a**, and **2b**−**4b** and related species in the "characteristic" regions of 3.5−6.5 and 7.5−10.0 ppm, which are not obscured by aliphatic or aromatic ligand signals. The agreement is seen to be quite good. Moreover, the calculations confirm that no other characteristic resonances should be observed for any of the products discussed here. Formation of pyridine N-alkylation products **6**, as reported recently for Li,[10] Mg, and Zn,[13] can be ruled out here both on the basis of their calculated NMR shifts and by comparison with the NMR data for the Mg and Zn analogues. The C3 (**7**) and imine-N (**8**) alkylation products are also calculated to have very characteristic shifts, allowing us to rule out their formation as well. In our opinion, calculation of NMR shifts can be a valuable tool in the assignment of spectra of mixtures.

Following the Reactions of 1 with Al Alkyls. The free ligand and aluminum alkyl (Me_3Al, Et_3Al, Et_2AlCl, $^{i}Bu_3Al$, or $^{i}Bu_2AlH$) were reacted in toluene (CH_2Cl_2 for $^{i}Bu_2AlH$). The solvent was then removed in vacuo, the residue was dissolved in toluene-d_8, and a spectrum was recorded. For Me_3Al and Et_2AlCl, the mixture was then sealed in an NMR tube, and spectra were recorded after keeping the sample for hours or days at elevated temperature. For Et_3Al, the main product (**3b**) was first isolated and sealed in an NMR tube in toluene-d_8, and its further rearrangements were followed by NMR. Table 3 lists the composition of the initial reaction mixture for all compounds, and Figure 4 summarizes the variations in concentration on heating.

In parallel experiments, EPR spectra were recorded of the reaction mixtures. These measurements indicated the presence

(21) See e.g.: (a) Satoh, H.; Koshino, H.; Uno, T.; Koichi, S.; Iwata, S.; Nakata, T. *Tetrahedron* **2005**, *61*, 7431. (b) Abraham, R. J.; Byrne, J. J.; Griffiths, L.; Koniotou, R. *Magn. Reson. Chem.* **2005**, *43*, 611, and references in these papers.

(22) See e.g.: Sefzik, T. H.; Turco, D.; Iuliocci, R. J.; Facelli, J. C. *J. Phys. Chem. A* **2005**, *109*, 1180, and references therein.

(23) Wolinski, K.; Hilton, J. F.; Pulay, P. *J. Am. Chem. Soc.* **1990**, *112*, 8251; Dodds, J. L.; McWeeny, R.; Sadlej, A. J. *Mol. Phys.* **1980**, *41*, 1419; Ditchfield, R. *Mol. Phys.* **1974**, *27*, 789; McWeeny, R. *Phys. Rev.* **1962**, *126*, 1028; London, F. *J. Phys. Radium (Paris)* **1937**, *8*, 397.

(24) Frisch, M. J.; Trucks, G. W.; Schlegel, H. B.; Scuseria, G. E.; Robb, M. A.; Cheeseman, J. R.; Zakrzewski, V. G.; Montgomery, J. A., Jr.; Stratmann, R. E.; Burant, J. C.; Dapprich, S.; Millam, J. M.; Daniels, A. D.; Kudin, K. N.; Strain, M. C.; Farkas, O.; Tomasi, J.; Barone, V.; Cossi, M.; Cammi, R.; Mennucci, B.; Pomelli, C.; Adamo, C.; Clifford, S.; Ochterski, J.; Petersson, G. A.; Ayala, P. Y.; Cui, Q.; Morokuma, K.; Rega, N.; Salvador, P.; Dannenberg, J. J.; Malick, D. K.; Rabuck, A. D.; Raghavachari, K.; Foresman, J. B.; Cioslowski, J.; Ortiz, J. V.; Baboul, A. G.; Stefanov, B. B.; Liu, G.; Liashenko, A.; Piskorz, P.; Komaromi, I.; Gomperts, R.; Martin, R. L.; Fox, D. J.; Keith, T.; Al-Laham, M. A.; Peng, C. Y.; Nanayakkara, A.; Challacombe, M.; Gill, P. M. W.; Johnson, B.; Chen, W.; Wong, M. W.; Andres, J. L.; Gonzalez, C.; Head-Gordon, M.; Replogle, E. S.; Pople, J. A. *Gaussian 98*, Revision A.11.4; Gaussian, Inc.: Pittsburgh, PA, 2002.

(25) Becke, A. D. *J. Chem. Phys.* **1996**, *104*, 1040.

(26) McLean, A. D.; Chandler, G. S. *J. Chem. Phys.* **1980**, *72*, 5639. Krishnan, R.; Binkley, J. S.; Seeger, R.; Pople, J. A. *J. Chem. Phys.* **1980**, *72*, 650.

(27) (a) Solvent effects are not included. Electronic solvent effects are expected to be small, but the preferred orientation of highly anisotropic solvent molecules such as benzene or toluene can still have large effects in particular on ^{1}H NMR shifts. (b) The molecules were optimized at a relatively low level (RI-bp86/SV(P), see computational details); optimization at a higher level was not feasible for these large species. (c) These molecules all have considerable conformational freedom. Exploring the full conformational space was not feasible, so we studied only a single conformation for each complex. This may be important in particular for ethyl complexes (where at least three conformations of each Et group should be considered) and for **2** (where the five-membered NAlNCC ring can pucker in different ways).

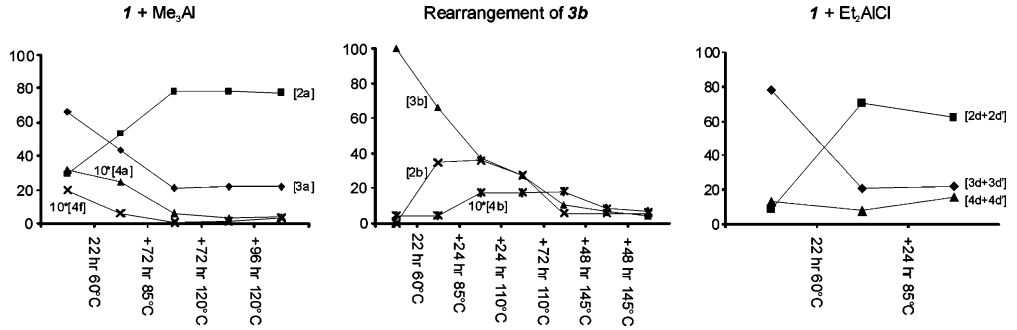

Figure 4. Changes in composition (mol %) of **1** + aluminum alkyl mixtures. Note the ×10 scale used for **4a**, **4f**, and **4b**.

of $LAlR_2$ radicals in amounts varying from 1% (Me_3Al) to ca. 0.01% ($^iBu_3Al$). These radicals have been discussed in a separate paper.[6] Gibson also noted formation of paramagnetic species in reactions of diimine pyridine ligands with alkylmagnesium and alkylzinc compounds.[13]

Reaction of Me_3Al with 1. The initial mixture showed formation of two major products, resulting from imine (**2a**) and C2 (**3a**) alkylation, formed in a ca. 1:2 ratio. In addition, small quantities of **4a** and **4f**[28] (ca. 2 mol % each) could be observed. On heating, **3a** slowly converted to **2a**, but the reaction appeared to stop at a **2a**:**3a** ratio of about 3:1; even prolonged heating did not cause further conversion. Complex **4f** already disappeared early in the reaction, while **4a** remained visible a little longer (both probably end up as dimers, as described below for other alkyls).

From these observations, we draw the following conclusions:

• C2 alkylation product **3a** is one of the initial reaction products, and it can rearrange to **2a**, most likely via reversion of the alkyl addition.

• The formation of **2a** from **3a** is too slow to explain the initial formation of ca. 30% of **2a**. This means that *either* **2a** is in part also an initial product (competing with **3a**) *or* conditions later on in the reaction are less favorable for converting **3a** to **2a** (possibly because the conversion is catalyzed by free Me_3Al, which at that time has been consumed).

• The final 3:1 **2a**:**3a** ratio might represent an equilibrium composition (at 120 °C), or it might be that the reaction stopped at this point because any factor that assisted the reaction at an earlier stage has disappeared at this point.

It seems clear that **3a** is a kinetic product, which for the largest part slowly converts to thermodynamically more stable **2a**, the product reported previously by Gibson.

Reaction of Et_3Al with 1. The initial reaction mixture here contained little of the imine alkylation product. Instead, the major products were **3b** and **4b**, in a ratio of about 2:1.[30] On heating, the concentration of **3b** slowly decreased and **2b** was formed as a major product. We monitored the behavior of purified **3b** on heating. On gentle heating, it partially converted to **2b** and a small quantity of **4b**. Prolonged heating at higher temperature did not change the ratio **2b**:**3b**, which remained close to 1:1. Instead, it resulted in slow decrease of *all* NMR signals attributable to derivatives of **1**.

Scheme 4. Diastereomeric Products that Could Be Formed from 1 and Et_2AlCl

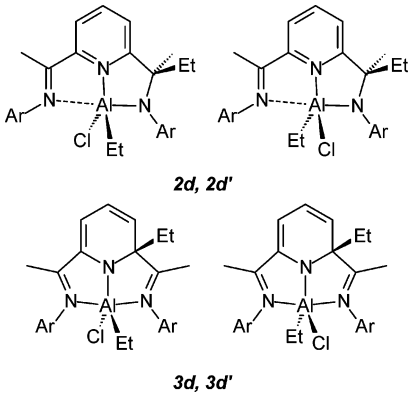

From these observations for Et_3Al we conclude the following:

• Complex **2b** can be formed via **3b**, like **2a** from **3a**. The surprise is that we now see hardly any *direct* formation of **2b**. Complex **4b** can be formed via **3b**; whether it can also be formed directly cannot be established with certainty.

• The most plausible explanation for the "stopping" of the conversion of **3b** to **2b** is the attainment of chemical equilibrium at a ca. 1:1 ratio; similarly, the above constant **2a**:**3a** ratio then most likely represents the equilibrium composition for the methyl case. It seems reasonable that steric hindrance would be more severe for alkylation at the imine carbon than at pyridine C2, and higher for ethyl than for methyl groups, which is consistent with the observed ratios (**2a**/**3a** > **2b**/**3b**).

The cause of the eventual decrease of the signals is not clear at present. Some solid material is formed, but not enough to explain the dramatic decrease in signal intensity. It could be that the eventual product is dimer **5b** of **4b** (we have never observed NMR signals for such dimers).

Reaction of Et_2AlCl with 1. The initial reaction mixture showed mainly pyridine ring alkylation to **3d** and **4d** (ca. 6:1); traces of a second isomer **3d′** of **3d** were also visible, as was about 9 mol % of **2d**. On heating, larger amounts of **2d**/**2d′** were formed, and the intensities of **3d** and **3d′** became similar. Conversion of **3d**/**3d′** to **2d**/**2d′** seemed to stop at a **2**:**3** ratio of about 3:1.

The formation of two isomers of **3d** and **2d** can reasonably be explained by partial exchange of the Et and Cl groups at Al to give diastereomers **3d′** and **2d′** as illustrated in Scheme 4.[31]

Even though preparative-scale experiments produced crystals of **5d**,[18] no resonances clearly attributable to this complex are observed in any of the spectra.

(28) The formation of **4f**, a product of *hydride* addition, is somewhat surprising here, since Me_3Al does not contain significant quantities of hydride impurities. One possible route is via *inter*moleculer transfer of the pyridine H4 from a molecule of **4a** to unreduced **1**, similar to the transfer we proposed to explain 1,4-dihydropyridyl formation from **1**·RhCl and Et_2Zn.[19] This type of hydrogen transfer is similar to the well-known addition of "a proton and two electrons" converting coenzyme NAD+ into NADH.[29]

(29) Stryer, L. *Biochemistry*, 4th ed.; W. H. Freeman: New York, 1995; pp 449−450.

(30) The amount of **4b** observed in the initial spectrum is somewhat variable. It may depend on speed of mixing, time required to measure the first spectrum, and other factors. However, the initial order of concentrations is always [**3b**] > [**4b**] > [**2b**].

(31) Disproportionation to $AlCl_2$ and $AlEt_2$ complexes would be expected to give even more complex spectra.

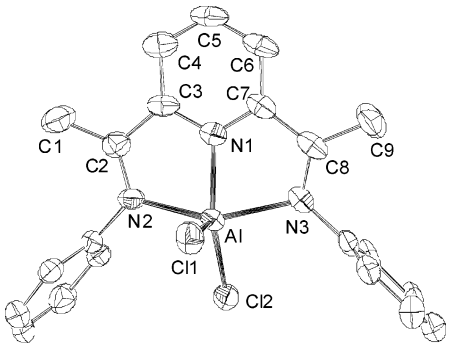

Figure 5. Thermal ellipsoid plot of the cation of **9** (50% probability). Hydrogen atoms and isopropyl groups are omitted for clarity.

Reaction of $^{i}Bu_3Al$ and $^{i}Bu_2AlH$ with 1. Spectra of the initial reaction mixture of $^{i}Bu_3Al$ and **1** showed formation of only very small amounts of alkylation products (ca. 6 mol % **4c** and 1 mol % **4e**). In addition, shifted ligand resonances were observed, which might indicate formation of one or more coordination complexes. On heating for longer periods, a precipitate was formed, which X-ray diffraction studies indicated to be the dimer **5e** of **4e**. The same dimer **5e** was prepared more conveniently from $^{i}Bu_2AlH$ and **1**. The spectrum from the latter reaction, directly after mixing the reagents in CH_2Cl_2 and evaporation of the solvent, showed mainly **4e** (judging from the characteristic triplets at 4.8 and 3.5 ppm) and no other recognizable complexes; workup after warming produced pure **5e**.

Reaction of $AlCl_3$ with 1. Heating **1** and $AlCl_3$ (1:1) in toluene produced an orange solution, from which two types of crystals deposited on cooling. One type looked like the free ligand; the other (complex **9**) was shown by X-ray diffraction (see below) to contain $[\mathbf{1}\cdot AlCl_2]^+$ cations and $AlCl_4^-$ anions. The NMR spectrum of a solution of these crystals shows clear but broadened low-field resonances for the pyridine H4 (8.77 ppm) and H3,5 (8.06) protons, which agree well with shifts calculated for the cation (Table 2).

Crystals of **9** contain two independent molecules as well as two molecules of toluene. Figure 5 and Table 6 refer to one of the cations; full details for all molecules in the structure can be found in the Supporting Information.

Computational Study of Alkylation and Dimerization. The observations described above demonstrate that the reaction of **1** with alkylaluminum compounds is quite complex. Addition can occur at different positions of the ligand (at least C2, C4, and imine C), and the products can undergo further reactions. Cation−anion pairs can also form, and this may be relevant to further reactivity. Therefore, we turned to theoretical methods (DFT) for a better understanding of this complex system. In particular, we wanted to understand the preferences for addition at various positions of the ligand and the nature of the unusual dimerization reaction. As a model system we used the reaction between simplified ligand **1′** (bearing only hydrogens at the imine carbon and nitrogen atoms) and Et_2AlCl.

Alkyl Addition to 1′. Preliminary studies revealed that after complexation of Et_2AlCl direct alkyl transfer to the pyridine C4 position has a very high barrier. This is hardly surprising, given the physical distance between the Al atom and the pyridine C4 position. Thus, more complicated mechanisms need to be considered for the formation of **4′**. One possibility might be

Scheme 5. Calculated Free Energies (kcal/mol; 273 K, 1 bar) of Minima and [Transition States], relative to 1′ + 2 Et_2AlCl

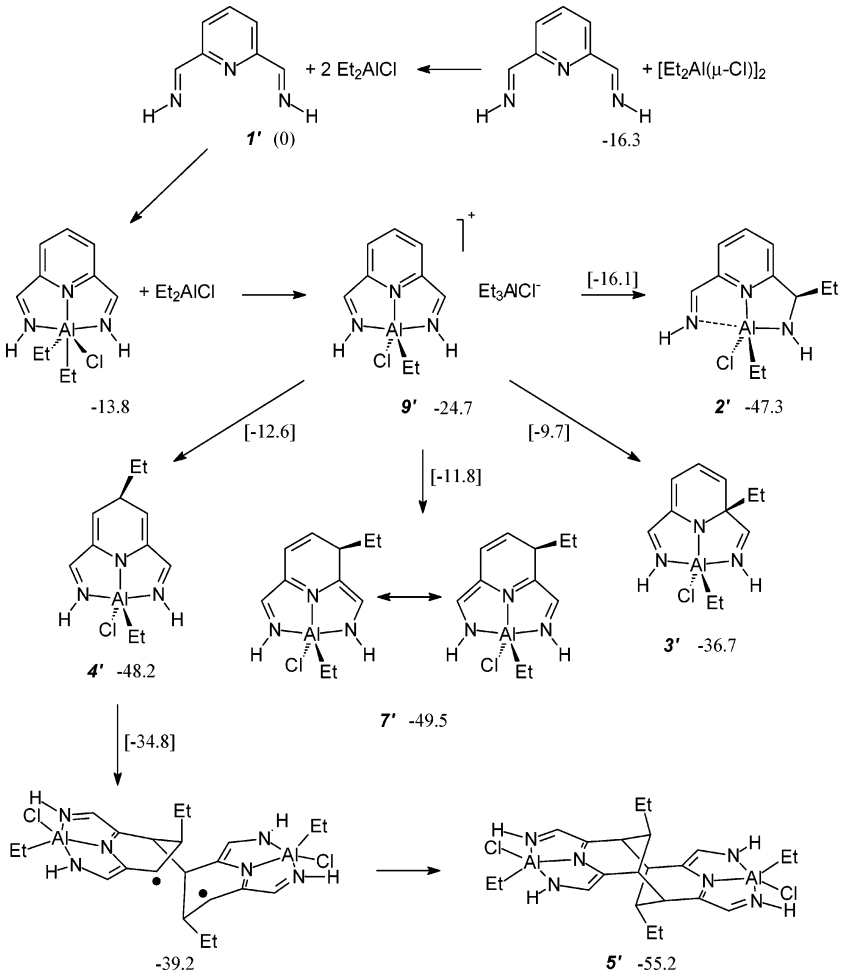

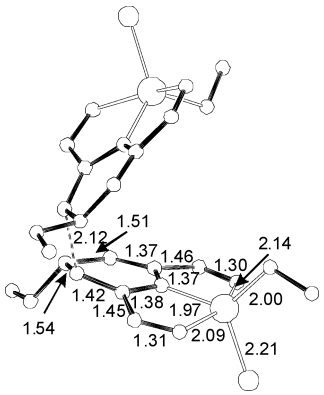

Figure 6. Bond distances in the transition state for the first C−C bond formation from two units of **4′**. Distances are symmetry averages over the two approaching monomers.

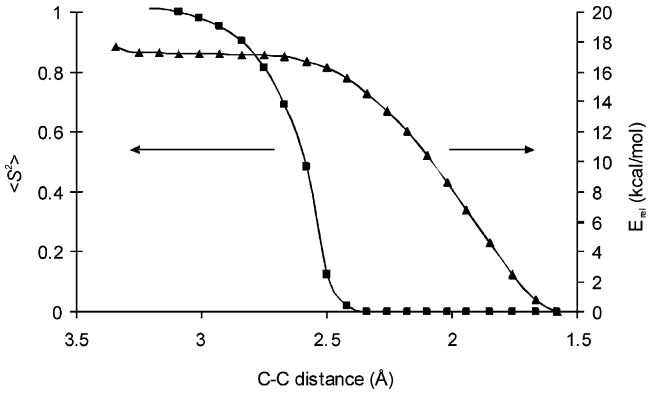

Figure 7. Energy profile for formation of the second C−C bond of **5′**: relative energy (▲) and $\langle S^2 \rangle$ value (■).

homolytic cleavage of an Al−C bond of **1**·AlR_3, followed by intra- or intermolecular transfer of the essentially free alkyl radical, comparable to the mechanism proposed for alkyl addition to α-diimine and Pyca systems.[14] We did indeed observe some formation of **1**·AlR_2 radicals, but it is not clear at present what their relation is to the observed diamagnetic products; they might also represent a side reaction. In any case, our observation of an ionic product **9** from **1** and $AlCl_3$ prompted us to consider the possibility of similar ionic species in our alkylations, and we decided to introduce a second molecule of Et_2AlCl in the calculations (all energies are therefore calculated relative to one ligand **1′** and 2 equiv of Et_2AlCl). This led to the reactions summarized in Scheme 5.

The loosely bound ion pair **9′** is calculated to be lower in energy than the separated molecules **1′** and $[Et_2AlCl]_2$ even in the gas phase.[32] Ethyl migration from the Et_3AlCl^- anion to various positions of the cation can now proceed smoothly: calculated free energy barriers are 15.0 (C2), 12.9 (C3), 12.1 (C4), and 8.6 (imine) kcal/mol. Transfer to C2 is mildly exothermic (12.0 kcal/mol); the other reactions are highly exothermic (24.8, 23.5, and 22.6 kcal/mol, respectively) and lead to products of comparable stability. However, steric hindrance present in the real ligand might make transfer to the imine position less favorable, as discussed later on.[33] The calculated barriers shown in the scheme are low enough to be compatible with initial alkylation via an ionic mechanism. Of course, this does not prove that the reaction of real ligand **1** with aluminum alkyls actually follows such an ionic path, but it seems that the ionic path can at least be a realistic alternative to the direct-transfer and free-radical paths.

Formation of Dimer 5′. At first sight, it seems reasonable to expect dimerization of **4′** to follow a more or less synchronous path for forming the two new C−C bonds. However, despite extensive searches such a symmetric path could not be located. Inspection of relevant orbitals shows that the symmetric approach is symmetry-forbidden, making a nonsynchronous biradical path likely. Indeed, we found that approach of two monomers of **4′** easily leads to *single* C−C coupling with a modest barrier of 13.4 kcal/mol (see Figure 6).

The resulting intermediate is essentially a biradical ($\langle S^2 \rangle$ = 1.01). After it has been formed, the two halves of the molecule rotate with respect to each other around the newly formed C−C bond to let the radical centers approach each other and so form the second C−C bond. The energy profile for this rotation is extremely flat. The final stages of the approach were followed by constrained geometry optimizations; Figure 7 shows the energy profile and the decrease in biradical character on giving final product **5′**. This is 30.5 kcal/mol below **9′** and 7.0 kcal/mol below **4′** and is probably the most stable product accessible from **9′**.

The symmetry-forbidden character of the direct, synchronous [3+3] dimerization path explains why we find a nonsynchronous biradical path for this reaction. It does not, however, explain the surprisingly low barrier we calculate for this nonsynchronous path. One possible explanation is the more efficient delocalization of negative charge over the two imine nitrogens in **5′** (in **4′**, it is formally localized on the pyridine nitrogen). In addition, **4′** is cross-conjugated, which is in general less favorable than the linear conjugation over the NCCNCCN path seen in **5′**. However, we do not believe that the calculated barrier of 13.4 kcal/mol for the biradical path is very accurate, since it is notoriously difficult to calculate accurate relative energies for open-shell and closed-shell species. Presumably, the most one can say on the basis of our calculations is that C−C coupling is "relatively easy".[34]

Relative Stabilities of the Various Alkylation Products. The above calculations on model compound **1′**, though useful in a qualitative sense, cannot be expected to accurately reproduce the relative stabilities of the various isomers in the crowded alkylation products derived from real ligand **1**. For more quantitative information, we optimized the complete structures of all possible products derived from Me_3Al and **1** (**2a**−**4a** and **6a**−**8a**) as well as the most relevant reaction products of Et_3Al (**2b**−**4b** and dimer **5b**). The resulting energies (Table 4) do not include thermal corrections, which would be too expensive for such large systems. Steric bulk is seen to have a major impact on the relative stabilities. It makes the imine and C2 alkylation products (**2** and **3**) comparable in energy and significantly higher than those of alkylation at C4 and C3 (**4** and **7**), which are also close to each other. The two products of N alkylation (**6** and **8**) are both much higher in energy. The change from Me_3Al to Et_3Al favors **3** over **2**, as expected. These calculated relative energies are consistent with the interpretation given earlier that the observed final ratios of **2** and **3** correspond to the equilibrium position. They are also compatible with eventual "disappearance" on heating of all of **2b**/**3b** via isomerization to the more

(32) Surprisingly, **9′** prefers a broken-symmetry electronic structure ($\langle S^2 \rangle$ = 0.28).

(33) The steric hindrance in **1** was earlier shown to have a large effect on the relative stabilities of iron dialkyl ligand alkylation products.[3]

(34) 1,4-Dihydropyridines bearing electron-withdrawing substituents easily undergo *photochemical* dimerization, even in the solid state. However, the structures of the [2+2] dimers thus obtained are very different from the [3+3] ones reported in the present work and refs 9 and 18. See e.g.: Hilgeroth, A.; Baumeister, U.; Heinemann, F. W. *Eur. J. Org. Chem.* **1998**, *1213*, 3.

stable **4b** and its subsequent dimerization to **5b**. However, neither the barriers shown in Scheme 5 nor the product stabilities listed in Table 4 explain why we have never observed any **7**, which is calculated to be as low in energy as **4** and equally easy to form. It might be that alkylation follows a path completely different from the ionic one studied here and that this alternative path has a large kinetic bias against attack at C3. Alternatively, it could be that **7** is even more reactive than **4** and rapidly dimerizes or polymerizes to nonobservable products.

Conclusions

The reaction of **1** with aluminum alkyls is surprisingly complex and features alkylation at the C2, C4, and imine carbons. These additions are in part reversible. The C4 alkylation product can dimerize to form the tricyclic ligand skeleton observed earlier for a chromium derivative.[9] Calculations indicate that for Al complexes **4** the dimerization follows a nonsynchronous biradical pathway; there seems to be no reason the chromium system would not follow the same route. The newly formed six-membered ring has all substituents in a well-defined stereoselective orientation, which suggests this reaction might have some potential in organic synthesis.

The mechanism(s) of ligand alkylation remain unclear. Direct alkyl transfer may play a role for imine and C2 alkylation but is unlikely for C4 alkylation. Transfer of free alkyl radicals is another possibility, although for the extremely reactive $CH_3^\bullet$ and $H^\bullet$ radicals one would expect many more side reactions. The calculations reported here show that an ionic mechanism is also a realistic possibility. Clearly, more work, both experimental and theoretical, is required before any possibility can be ruled out.

Experimental Section

General Procedures. All manipulations were carried out under an atmosphere of argon using standard Schlenk techniques or in a conventional nitrogen-filled glovebox. Solvents were refluxed over an appropriate drying agent and distilled prior to use. NMR spectra were recorded on Varian and Bruker spectrometers at ambient temperature. For NMR spectra of mixtures, only clearly separated signals are reported here.

1 + Me$_3$Al. Light yellow **1** (218 mg, 453 μmol) was suspended in 5 mL of toluene. Me_3Al was added (65.3 μL, 679 μmol; 1.5 equiv), which resulted in the formation of a yellow-brown solution. The solution was evaporated to dryness, and a ^{1}H NMR spectrum was recorded in C_7D_8, after which the NMR tube was sealed. ^{1}H NMR spectra at room temperature were recorded again after heating at 60 °C for 22 h, after heating at 85 °C for 72 h, after heating at 120 °C for 72 h, and after heating at 120 °C for a final 96 h. The following signals could be assigned (part of the ^{1}H NMR data is from a separate experiment and recorded in C_6D_6, where COSY and NOESY data allowed a more complete assignment; assignments for **2a** were verified by comparison with an authentic sample of pure **2a**[11]):

2a. ^{1}H NMR (400 MHz, C_6D_6): δ 3.97, 2.94 (sept, 2H each, $^3J_{HH}$ = 6.8 Hz, C*H*(CH$_3$)$_2$), 1.67 (s, 3H, N=CC*H*$_3$), 1.46 (s, 6H, NC(C*H*$_3$)$_2$), 1.39, 1.38, 1.32, 0.97 (d, 6H each, $^3J_{HH}$ = 6.8 Hz, CH(C*H*$_3$)$_2$), −0.52 (s, 6H, Al(C*H*$_3$)$_2$). ^{13}C NMR (50 MHz, C_6D_6): δ 174.0 (N=*C*CH$_3$) 163.1 (Py *C*6), 155.6 (Py *C*2) 62.0 (N*C*(CH$_3$)$_2$), −4.0 (Al(*C*H$_3$)$_2$).

3a. ^{1}H NMR (400 MHz, C_6D_6): δ 6.32 (dd, 1H, $^3J_{HH}$ = 6.0 and 8.8 Hz, Py *H*4), 5.74 (dd, 1H, $^3J_{HH}$ = 6.0 Hz, $^4J_{HH}$ = 0.6 Hz, Py *H*5), 5.16 (dd, 1H, $^3J_{HH}$ = 8.8, $^4J_{HH}$ = 0.6 Hz, Py *H*3), 3.16, 3.07, 3.04, 2.89 (sept, 1H each, $^3J_{HH}$ = 6.8 Hz, C*H*(CH$_3$)$_2$), 1.77, 1.52 (s, 3H each, N=CC*H*$_3$), 1.39, 1.35, 1.34, 1.32, 1.00, 0.94, 0.85, 0.85 (d, 3H each, $^3J_{HH}$ = 6.8 Hz, CH(C*H*$_3$)$_2$), −0.43, −0.66 (s, 3H each, AlC*H*$_3$).

4a. ^{1}H NMR (400 MHz, C_7D_8): δ 5.03 (d, 2H, $^3J_{HH}$ = 3.8 Hz, Py *H*3,5) 3.52 (m, 1H, Py *H*4).

4f. ^{1}H NMR (400 MHz, C_7D_8): δ 4.94 (t, 2H, $^3J_{HH}$ = 3.8 Hz, Py *H*3,5) 3.53 (t, 2H, $^3J_{HH}$ = 3.8 Hz, Py *H*4).

Synthesis of 3b. To 0.296 g of **1** (0.615 mmol) in 3 mL of hexane was added 0.74 mL of 1 M Et$_3$Al in hexanes, which resulted in a color change from yellow to green. The suspension was stirred overnight at room temperature, after which it was cooled to −30 °C for one week. It was filtered, and the orange-yellow residue was washed with 5 mL of ice-cold hexane and dried in vacuo. ^{1}H NMR showed that this was pure **3b**, of which all peaks could be assigned; yield 0.044 g (12%).

3b. ^{1}H NMR (400 MHz, C_6D_6): δ 7.11−7.07 (m, 6H, Ar *H*), 6.29 (dd, 1H, $^3J_{HH}$ = 5.8 and 8.8 Hz, Py *H*4), 5.66 (dd, 1H, $^3J_{HH}$ = 5.8 Hz, $^4J_{HH}$ = 0.7 Hz, Py *H*5), 5.12 (dd, 1H, $^3J_{HH}$ = 8.8 Hz, $^4J_{HH}$ = 0.7 Hz, Py *H*3), 3.21, 3.09, 3.07, 3.01 (sept, 1H each, $^3J_{HH}$ = 6.8 Hz, C*H*(CH$_3$)$_2$), 2.45−2.36, 1.31−1.23 (m, 1H each, Py-C2-C*H*$_2$CH$_3$), 1.74, 1.55 (s, 3H each, N=CC*H*$_3$), 1.41 (2×), 1.39, 1.37, 1.11, 1.00, 0.99, 0.97 (d, 3H each, $^3J_{HH}$ = 6.8 Hz, CH(C*H*$_3$)$_2$), 1.19, 0.73 (t, 3H each, $^3J_{HH}$ = 8.0 Hz, AlCH$_2$C*H*$_3$), 0.90 (t, 3H, $^3J_{HH}$ = 8.0 Hz, Py-C2-CH$_2$C*H*$_3$), 0.23−0.09, 0.10−0.02 (m, 2H each, AlC*H*$_2$CH$_3$). ^{13}C NMR (50 MHz, C_6D_6): δ 183.1, 173.8 (N=*C*CH$_3$) 146.2, 143.2, 143.0, 141.1, 140.5, 140.0 (2×) (Py *C*6, Ar C_i, Ar C_o), 126.7, 126.5, 124.6, 124.5, 124.4, 123.8 (Ar C_m, Ar C_p), 126.2 (Py*C*4), 114.2 (Py *C*5), 101.7 (Py *C*3), 67.5 (Py *C*2), 28.6, 28.3, 27.7 (2×), 27.5 (*C*H(CH$_3$)$_2$), Py-C2-*C*H$_2$CH$_3$), 26.0, 25.4, 25.0 (2×), 24.9, 24.1, 23.7, 23.1 (CH(*C*H$_3$)$_2$), 17.9, 16.8 (N=C*C*H$_3$), 10.8, 8.7 (AlCH$_2$*C*H$_3$), 6.2 (Py-C2-CH$_2$*C*H$_3$), 1.4, −0.5 (Al*C*H$_2$CH$_3$). Anal. Calcd (%) for $C_{39}H_{58}N_3Al$: C 78.61, H 9.81, N 7.05. Found: C 78.74, H 9.05, N 7.87.

Heating of 3b. Spectra were recorded after heating a sealed C_7D_8 solution of pure **3b** at 60 °C for 22 h, at 85 °C for another 24 h, at 110 °C for another 24 h, at 110 °C for another 72 h, at 145 °C for another 48 h, and at 145 °C for a final 48 h. Apart from **3b** (vide supra) the following signals could be assigned:

2b. ^{1}H NMR (200 MHz, C_6D_6): δ 4.38 (sept, 1H, $^3J_{HH}$ = 6.8 Hz, C*H*(CH$_3$)$_2$) (assignments verified by comparison with an authentic sample of pure **2b**[11]).

4b. ^{1}H NMR (400 MHz, C_6D_6): δ 5.03 (d, 2H, $^3J_{HH}$ = 3.8 Hz, Py *H*3,5), 3.70−3.65 (m, 1H, Py *H*4), 1.70 (s, 6H, N=CC*H*$_3$).

Crystallization of 3b. In a separate experiment 0.26 g of **1** (0.55 mmol) was suspended in 10 mL of toluene at −50 °C, and 0.6 mL of 1 M Et$_3$Al in hexanes (0.60 mmol; 1.1 equiv) was added, which resulted in a color change from yellow to light orange. Warming up to room temperature resulted in a darkening of this color. On slow evaporation crystals were grown, which were suitable for X-ray diffraction.

1 + Et$_2$AlCl. To 0.140 g of **1** (291 μmol) in 5 mL of toluene was added 0.34 mL of a ca. 1 M solution of Et$_2$AlCl in hexanes (336 μmol, 1.16 equiv), which resulted in a color change from yellow to yellow-green. The solution was evaporated to dryness, redissolved in C_7D_8, and sealed in an NMR tube. A ^{1}H NMR spectrum was recorded immediately, then after heating 22 h at 60 °C (solution has become yellow-brown) and after 24 h at 85 °C (solution has become brown). Spectra recorded after further heating were broad and featureless. The following signals could be assigned:

2d. ^{1}H NMR (300 MHz, C_7D_8): δ 4.52 (sept, 1H, $^3J_{HH}$ = 6.8 Hz, C*H*(CH$_3$)$_2$).

3d. ^{1}H NMR (300 MHz, C_7D_8): δ 6.12 (dd, 1H, $^3J_{HH}$ = 5.8 and 8.8 Hz, Py *H*4), 5.56 (d, 1H, $^3J_{HH}$ = 6.0 Hz, Py *H*5), 5.16 (d, 1H, $^3J_{HH}$ = 9.0, Py *H*3), 1.72, 1.56 (s, 3H each, N=CC*H*$_3$) 0.74 (t, 3H, $^3J_{HH}$ = 8.0 Hz, AlCH$_2$C*H*$_3$), 0.10 (quart, 2H, $^3J_{HH}$ = 8.0 Hz, AlC*H*$_2$-CH$_3$).

4d. ^{1}H NMR (300 MHz, C_7D_8): δ 5.10 (d, 2H, $^3J_{HH}$ = 3.8 Hz, Py *H*3,5).

1 + *i*Bu$_3$Al. To 0.214 g of **1** (444 mmol) in 5 mL of toluene was added 0.367 g of 1 M ^{i}Bu$_3$Al (1.19 equiv), which resulted in a color change from yellow to brown. The solution was evaporated to dryness, redissolved in C_7D_8, and sealed in an NMR tube. A ^{1}H NMR spectrum was recorded immediately. The solution changed color on heating (first to red and then to purple-red), but spectra recorded after heating showed mostly broad lines and were not readily interpretable; purple crystals formed from the solution after heating proved to be **5e** (X-ray). In the initial spectrum, the following signals could be assigned:

4c. ^{1}H NMR (400 MHz, C_6D_6): δ 5.09 (d, 2H, $^3J_{HH}$ = 4.1 Hz, Py *H*3,5), 3.81−3.73 (m, 1H, Py *H*4).

4e. ^{1}H NMR (400 MHz, C_6D_6): δ 4.87 (t, 2H, $^3J_{HH}$ = 3.8 Hz, Py*H*3,5), 3.54 (t, 2H, $^3J_{HH}$ = 3.8 Hz, Py *H*4).

1 + *i*Bu$_2$AlH. To 0.505 g of **1** (1.05 mmol) in 10 mL of hexane was added 1.15 mL of 1 M ^{i}Bu$_2$AlH (1.10 equiv), which resulted in a color change from yellow to green. Crystals formed from this solution on cooling proved to be green **4e** (X-ray; for details see Supporting Information). The solution was heated at 110 °C for 2 h, which resulted in a color change to purple. After cooling overnight, 70 mg (10.7%) of crystals suitable for X-ray diffraction had formed; they were identified as **5e**, identical to the crystals formed from ^{i}Bu$_3$Al, by comparison of the observed and calculated powder diffraction patterns. Unfortunately, the poor solubility of the product did not allow recording of NMR spectra. The clearest initial ^{1}H NMR spectrum was obtained by mixing **1** and ^{i}Bu$_2$AlH in CH_2Cl_2, removing the solvent and then recording the spectrum in toluene-d_8; data in Table 3 are based on such a spectrum. Anal. Calcd (%) for $C_{82}H_{124}N_6Al_2$ (**5e**): C 78.93, H 10.02, N 6.73, Al 4.32. Found: C 78.64, H 9.90, N 6.84, Al 4.22.

1 + AlCl$_3$. To 224 mg of **1** (yellow, 0.47 mmol) were added 62 mg of $AlCl_3$ (yellow; 0.465 mmol; 1.0 equiv) and 15 mL of toluene, which resulted in a light orange suspension. This was heated to 87 °C and then slowly cooled, upon which two types of crystals formed: small yellow needles that looked liked free ligand, as well as larger shiny yellow-orange cubes that were structurally characterized as **9**.

9. ^{1}H NMR (200 MHz, C_6D_6): δ 8.63 (t, 1H, $^3J_{HH}$ = 7.7 Hz, Py *H*4), 7.92 (d, 2H, $^3J_{HH}$ = 7.7 Hz, Py *H*3,5), 7.17−7.02 (m, 6H, Ar *H*), 2.88 (sept, 4H, $^3J_{HH}$ = 6.6 Hz, C*H*(CH$_3$)$_2$), 2.03 (s, 6H, N=CC*H*$_3$), 1.33, 1.03 (d, 12H each, $^3J_{HH}$ = 6.6 Hz, CH(C*H*$_3$)$_2$). Anal. Calcd (%) for $C_{33}H_{43}N_3Cl_6Al_2 \cdot C_7H_8$: C 57.16, H 6.12, N 5.00, Cl 25.31. Found: C 56.96, H 6.13, N 5.09, Cl 25.53.

Structure Determination of 2a, 3b, 5e, and 9. The molecular structures of **2a**, **3b**, **5e**, and **9** were determined by single-crystal X-ray diffraction. For measurement of **3b**, the crystal was mounted in a glass capillary. The structures were solved by the PATTY option[35] of the DIRDIF program system.[36] Notes on individual structures follow.

2a. The structure contains one cocrystallized molecule of toluene in a general position and one molecule of toluene located over an inversion center. Although the geometry of the Al complex is quite acceptable, the geometries of the toluene solvent molecules certainly are not. The toluene molecule in a general position had to be constrained rather strictly in order to keep the geometry acceptable. The other toluene molecule has a symmetry-imposed disorder; we did not locate or calculate hydrogen positions for this solvent molecule. As a consequence, the thermal displacement parameters of the toluene molecules are rather large, and no conclusions may be derived based on these molecules. Nevertheless, we are convinced that the connectivity and geometry of the Al complex are correct and accurate enough.

3b. The unit cell contains two independent molecules with only minor geometrical differences.

5e. The asymmetric unit consists of only half a molecule, since the dimer is positioned around an inversion center.

9. This structure, like that of **3b**, contains two crystallographically independent molecules. In addition, one molecule of toluene per **9** was found to be present in the lattice. The crystal structure determination of **9** was hampered by the poor crystal quality. Some of the chlorine atoms of the $AlCl_4$ moieties show large molecular displacement parameters, even though the data were collected at −65 °C. It proved to be impossible to describe this disorder; all attempts to do so led to unstable refinements. The same holds to a lesser extent for one of the isopropyl CH_3 carbons and one of the *ipso* carbons of a diisopropylphenyl group. The four highest peaks in the difference Fourier map (1.76 to 1.14 e/Å^3) are all close to the above-mentioned chlorine atoms; the fifth peak is only 0.40 e/Å^3.

The crystal data and a summary of the data collection and structure refinement for all four structures are given in Table 5. The structure and part of the atomic numbering is shown in Figures 1 (**2a**), 2 (**3b**), 3 (**5e**), and 5 (**9**).[37] A selection of bond distances and angles is given in Table 6. Complete crystallographic data (CIF) are provided as Supporting Information. A drawing of **4e** and details of the low-quality structure determination for this compound are given in the Supporting Information.

Calculations. All geometry optimizations were carried out with the Turbomole program[38,39] coupled to the PQS Baker optimizer.[40,41] Geometries were fully optimized as minima or transition states at the unrestricted (for **1′**) or restricted (for **1**) bp86[42,43]/RIDFT[44] level using the Turbomole SV(P) basis set[45] on all atoms. For model system **1′** bearing only hydrogens at the imine carbon and nitrogen, all stationary points were characterized by vibrational analyses (numerical frequencies); ZPE and thermal (enthalpy *and* entropy) corrections (1 bar, 273 K) from these analyses are included. For these systems, all energies mentioned in text and tables are free energies. For the full systems derived from **1**, Gaussian98[24] was used to calculate chemical shifts using the GIAO formalism,[23] the B3LYP functional,[25] and the 6-311G** basis.[26] Thermal corrections were not feasible for these larger systems.

Supporting Information Available: Complete crystallographic data (CIF format) for complexes **2a**, **3b**, **5e**, **9**, and **4e**; ^{1}H NMR

(35) Beurskens, P. T.; Beurskens, G.; Strumpel, M.; Nordman, C. E. In *Patterson and Pattersons*; Glusker, J. P., Patterson, B. K., Rossi, M., Eds.; Clarendon Press: Oxford, 1987; p 356.

(36) Beurskens, P. T.; Beurskens, G.; Bosman, W. P.; de Gelder, R.; Garcia-Granda, S.; Gould, R. O.; Israel, R.; Smits, J. M. M. *DIRDIF-96*. A computer program system for crystal structure determination by Patterson methods and direct methods applied to difference structure factors; Crystallography Laboratory, University of Nijmegen: The Netherlands, 1996.

(37) Spek, A. L. *PLATON*. A Multipurpose Crystallographic Tool; Utrecht University: Utrecht, The Netherlands, 2003.

(38) Ahlrichs, R.; Bär, M.; Baron, H.-P.; Bauernschmitt, R.; Böcker, S.; Ehrig, M.; Eichkorn, K.; Elliott, S.; Furche, F.; Haase, F.; Häser, M.; Hättig, C.; Horn, H.; Huber, C.; Huniar, U.; Kattannek, M.; Köhn, A.; Kölmel, C.; Kollwitz, M.; May, K.; Ochsenfeld, C.; Öhm, H.; Schäfer, A.; Schneider, U.; Treutler, O.; Tsereteli, K.; Unterreiner, B.; Von Arnim, M.; Weigend, F.; Weis, P.; Weiss, H. *Turbomole* Version 5; Theoretical Chemistry Group, University of Karlsruhe: Germany, January 2002.

(39) Treutler, O.; Ahlrichs, R. *J. Chem. Phys.* **1995**, *102*, 346.

(40) *PQS* version 2.4; Parallel Quantum Solutions: Fayetteville, AR, 2001 (the Baker optimizer is available separately from PQS upon request).

(41) Baker, J. *J. Comput. Chem.* **1986**, *7*, 385.

(42) Becke, A. D. *Phys. Rev. A* **1988**, *38*, 3089.

(43) Perdew, J. P. *Phys. Rev. B* **1986**, *33*, 8822.

(44) Eichkorn, K.; Weigend, F.; Treutler, O.; Ahlrichs, R. *Theor. Chem. Acc.* **1997**, *97*, 119.

(45) Schaefer, A.; Horn, H.; Ahlrichs, R. *J. Chem. Phys.* **1992**, *97*, 2571.

(46) Sheldrick, G. M. *SADABS*, Program for Empirical Absorption Correction; University of Göttingen: Germany, 1996.

(47) Sheldrick, G. M. *SHELXL-97*, Program for the refinement of crystal structures; University of Göttingen: Germany, 1997.

spectra for the reaction between **1** and $AlMe_3$ (Figure S1), Et_2AlCl (Figure S3), and the heating of **3b** (Figure S2); molecular structure (Figure S4) and crystallographic details (Table S1) for the low-quality X-ray structure determination of **4e**; total energies and thermal corrections for geometries of minima and transition states derived from **1′** as calculated by DFT (Table S2); selected bond distances for these species (Figures S5−S7); calculated total energies for **2a**−**4a**, **6a**−**8a**, and **2b**−**4b** at RIDFT-bp86/SV(P) and B3LYP/6-311G** levels (Table S3), and calculated NMR chemical shifts for various alkylation products and coordination complexes of **1**. This material is available free of charge via the Internet at http://pubs.acs.org.

OM050936M